



Contents lists available at ScienceDirect

## Discrete Applied Mathematics

journal homepage: [www.elsevier.com/locate/dam](http://www.elsevier.com/locate/dam)

# Modeling the process of human body iron homeostasis using a variant of timed Petri nets<sup>☆</sup>

Jacek Blazewicz<sup>a,c</sup>, Dorota Formanowicz<sup>b</sup>, Piotr Formanowicz<sup>a,c,\*</sup>, Andrea Sackmann<sup>a</sup>, Michał Sajkowski<sup>a</sup><sup>a</sup> Institute of Computing Science, Poznań University of Technology, Piotrowo 2, 60-965 Poznań, Poland<sup>b</sup> Department of Clinical Biochemistry, Poznań University of Medical Sciences, Grunwaldzka 6, 60-780 Poznań, Poland<sup>c</sup> Institute of Bioorganic Chemistry, Polish Academy of Sciences, Noskowskiego 12/14, 61-704 Poznań, Poland

## ARTICLE INFO

## Article history:

Received 7 January 2007

Received in revised form 13 June 2007

Accepted 11 June 2008

Available online xxxx

## Keywords:

Petri net model  
Iron homeostasis  
Net analysis  
Time dependence

## ABSTRACT

The body iron homeostasis is one of the most important processes in the human body. This complex process is not fully understood and until recently only some parts of it have been described in the literature. In our recent papers the main part of the process has been described and a model based on Petri net theory has been proposed. However, in this model any time dependencies occurring in the biochemical process have not been taken into account. In the present paper the model is enriched in the way that durations of biochemical reactions composing this process have been included into the model. A variant of Petri net where with each place a time interval is associated has been used in order to describe these dependencies. The time interval associated with a place corresponds to a time lag of biochemical conditions which must be fulfilled in order to enable a biochemical reaction to start.

© 2008 Elsevier B.V. All rights reserved.

## 1. Introduction

In this paper an extension of the recently proposed model of the human body iron homeostasis is proposed. This complex process plays a crucial role in the human body but it is not fully understood. Until recently, only some components of it have been described in the literature. These descriptions have been given in a rather informal way, i.e. they were not expressed in a language of any mathematical theory. From this follows that they were not very precise. In a series of our recent papers [2–4] the main part of this important process has been described and its model has been formulated in the language of Petri net theory. The model has been analyzed in detail in [3]. However, since for this modeling, a Petri net without time information has been used, the model does not contain any information about time dependencies which are present in the real process and may be crucial for understanding its nature. Although they are not known precisely, they can be estimated by time intervals. In the present paper the core of the model is extended by adding to it time durations of biochemical reactions composing the process. These time durations are modeled by time intervals associated with every place in the net. They should be interpreted as time spans in which the time points of the fulfillment of some biochemical conditions, necessary to enable some biochemical reactions to start, lie. This extension makes the model more realistic since it takes into account more features of the analyzed biochemical process than the previous model, where the time dependencies occurring in the studied phenomenon were not considered.

<sup>☆</sup> This research has been partially supported by the EU grant Bioptrain and by the Polish Ministry of Science and Higher Education.<sup>\*</sup> Corresponding author at: Institute of Computing Science, Poznań University of Technology, Piotrowo 2, 60-965 Poznań, Poland. Fax: +48 61 8771525. E-mail address: [piotr@cs.put.poznan.pl](mailto:piotr@cs.put.poznan.pl) (P. Formanowicz).

Iron is one of the key components of many important biological processes in the human body. It is crucial for many cellular functions and for the proper growth and development of tissues. On the other hand, natural iron is insoluble and can catalyze the formation of potentially damaging toxic oxygen radicals. Hence, an excess of iron may lead to serious diseases. Since humans have a very limited capacity of excreting iron, cells have developed mechanisms of improving iron solubility to control the iron concentrations. However, the signaling pathways and the molecular components involved in this control process are not very well understood. First attempts to build a precise model of it have been made in [2–4]. In the present paper an extension of the central part of the model is presented in the language of a variant of timed Petri net.

The Petri nets have been proposed in 1962 by Carl A. Petri in the context of technical systems [5]. Different kinds of such systems were the main area of Petri net applications until the last decade of the 20th century. With the rapid growth of computational biology Petri nets have been also used to model biological systems (cf. [6,7]). Nowadays, they are used for modeling and analyzing various biological processes, e.g. metabolic pathways (cf. [8]), gene regulatory networks (cf. [9]) and signal transduction pathways (cf. [10]). For an overview of biological applications of Petri nets see [11,12].

The analysis approach presented in this paper is mainly based on the net invariants. The definition of these invariants was introduced in [13]. The first biological application of minimal  $t$ -invariants to analyze metabolic networks in the steady state was introduced in [14] in the form of elementary modes. In [15] the invariant analysis is proposed and discussed as a validation of a qualitative Petri net model.

The organization of the paper is as follows. In Section 2 the human body iron homeostasis process is described. In Section 3 definitions of the Petri net and its extension used to model the considered biochemical process are presented and analyzed. In Section 4 the Petri net based model of the homeostasis process is analyzed. The paper ends with conclusions in Section 5.

## 2. Human body iron homeostasis

Iron is an ubiquitous element in the environment and in biology, essential for nearly all living organisms, including human [16]. The mechanisms and factors that influence and regulate human body iron homeostasis are very complicated and still not fully understood phenomena.

After absorption in the small intestine, iron ( $\text{Fe}^{3+}$ ) binds to serum transferrin (Tf). This protein is responsible for its transport from the sites of absorption and storage to the various cells having transferrin receptor-1 (TfR1) on their surface [17]. As a result of this process (i.e. binding Tf( $\text{Fe}^{3+}$ ) to TfR1) comes into being a complex which is internalized by the receptor mediated endocytosis (RME) into cellular endosomes. Tf binds to the TfR in 2:2 (Tf: TfR subunit) stoichiometry [18]. After the internalization of this complex, iron  $\text{Fe}^{3+}$  is released from Tf under the endosomal acidic conditions and occurs in the reduced form as  $\text{Fe}^{2+}$ . Then, in this form iron is transported into the cytosol or mitochondria of the all-proliferative cells (among others the one-nuclear cells, the preerythrocytes and the erythrocytes) and reaches their labile iron pool (LIP) [19].

The LIP is regulated in the most of the cells by iron responsive proteins (IRPs) that sense its level, and in turn control the translation of the TfR and the ferritin in a compensatory manner. A rise in Fe uptake increases the LIP and results in the IRPs inactivation. The latter concomitantly evokes the ferritin synthesis and blocks the TfR synthesis by inducing the TfR mRNA degradation. The LIP is the compartment from which iron is either metabolically drawn into Fe-dependent enzymes, transported into mitochondria for the heme synthesis or incorporated into the ferritin for a secure storage and/or detoxification. How LIP acts depends on the body iron status. If there is a low concentration of the serum iron in the human body, the iron ( $\text{Fe}^{2+}$ ) from the one-nuclear cells LIP is mostly transported out by the protein called ferroportin (Fpn). If the concentration of the serum iron in the human body is high, the iron from the one-nuclear cells LIP is mostly transported out into the ferritin, which acts as the human body iron storage [19].

The erythroid precursors (preerythrocytes) and the red blood cells are other cells, apart from the one-nuclear cells, involved in the body iron homeostasis. In case of these cells, the majority of iron which enters them is transported into mitochondria for the heme synthesis. This phenomenon increases especially due to anemia, when the serum red blood cells and serum iron concentrations are insufficient for the proper function of the human body. In this case synthesis of erythropoietin (EPO), the hormone produced by the kidneys is increased to enhance the erythrocytes production. The red blood cells live in the human body about 120 days and after that period of time they are phagocytosed by the one-nuclear cells. These cells are responsible for the recirculation of the iron derived from the effete red cells so that it may enter the circulation, bind to the Tf, and be transported to the bone marrow for the red blood cells production [20].

The body iron metabolism is changing under the influence of the inflammatory process. It is generally thought that the inflammation alters the one-nuclear cells iron homeostasis, resulting in an increased iron retention and a reduced iron release, thus giving rise to the low iron concentration and anemia, although in the latter event defects in the red blood cells production may be also involved [21].

A protein whose production is modulated in response to the inflammation, the anemia and the hypoxia is the hepcidin [22]. Recently, it has been found that this protein regulates the cellular iron efflux by binding it to the Fpn [23,24]. In the latter phenomenon of inflammatory-induced hepcidin expression, causing an Fpn degradation might account for the iron sequestration within the one-nuclear cells. The influence of the inflammatory process on the human body iron homeostasis what has been described in detail in [4]. In a recently suggested model, for the regulation of the hepcidin expression, the hepatocyte surface HFE (the hemochromatosis protein) competes with the HoloTf( $\text{Fe}^{3+}$ ) for the binding with TfR1, which is the transferrin receptor-2 (TfR2) competitor [24]. The unbound surface of the HFE and a higher concentration of Tf( $\text{Fe}^{3+}$ )-TfR2 complex were proposed to increase the hepcidin expression and its release. According to this model, the iron deficiency

would lead to a decrease of the circulating Tf( $\text{Fe}^{3+}$ ) and an increase of the number of free surface TfR1s, resulting in a lower concentration of the Tf( $\text{Fe}^{3+}$ )-TfR2 complex and the decreased fraction of the free surface of the HFE. The main part of the human body iron homeostasis process has been described in more detail in [2].

### 3. Petri net models

In this section an introduction to Petri nets is given firstly by a short repetition of some basic definitions of Petri nets. For a more detailed introduction see [25] or [26], respectively. Afterwards a variant of Petri nets where some information about time dependencies in the modeled process are taken into account is presented.

#### 3.1. Definitions

Petri nets are bipartite digraphs, i.e. they consist of two disjoint sets of nodes and directed arcs connecting only nodes of different sets. One set of nodes is called the places which typically model the passive components of the system as conditions or biological compounds which are represented by circles. The fulfillment of a condition or the presence of a compound, respectively, is indicated by tokens residing in places. Generally, each place in a discrete Petri net may carry any non-negative integer number of tokens. To restrict the number of tokens at a place it can get a capacity which then is an integer limit of the token number which cannot be exceeded.

The other set of nodes is given by the transitions representing the active system elements as events or biological reactions. In graphical representations transitions are depicted as rectangles.

More formally, a Petri net is a 5-tuple [27]  $N = (P, T, I, O, M_0)$ , where:

- $P = \{p_1, p_2, \dots, p_m\}$  is a finite set of places,
- $T = \{t_1, t_2, \dots, t_n\}$  is a finite set of transitions,  $P \cup T \neq \emptyset$  and  $P \cap T = \emptyset$ ,
- $I : (P \times T) \rightarrow \mathbb{N}$  is an input function that defines directed arcs from places to transitions,
- $O : (T \times P) \rightarrow \mathbb{N}$  is an output function that defines directed arcs from transitions to places and
- $M_0 : P \rightarrow \mathbb{N}$  is the initial marking.

The arcs indicate the relation between the active and the passive system components. Generally, Petri nets are multigraphs. The parallel arcs of a multigraph can be modeled by arc weights in a graph – see the input and output functions above – but here we only refer to ordinary nets, i.e. all arcs are weighted with one. Depending on the arc direction the adjacent places of a transition are discriminated as its pre- and post-places. If all of its pre-places are sufficiently marked with tokens a transition is enabled to fire. With its firing it removes a token from each pre-place and puts one at each of its post-places. Thus, the tokens are the dynamic element of the Petri net. Generally, their number in the net is not conserved since the number of a transition's pre-places has not to be equal to the number of its post-places. If a pre-place has to be marked with tokens but with a firing of its adjacent transition any token is not removed from the place, these nodes (i.e. the place and the transition) are connected via two converse arcs. They are depicted as bidirectional arrows and are called *read arcs*.

As named above  $M_0 : P \rightarrow \mathbb{N}$  defines the initial marking of the net, i.e. the distribution of the tokens over all places characterizing the current state of the system. The initial marking is given before any transitions have fired and it defines the system state assumed to be the physiologically normal one (in the case of the considered biochemical system). The set of reachable markings consists of all markings which are reachable from the initial marking by the successive firing of a transitions sequence. The *reachability graph* of a Petri net contains all reachable markings as nodes. A directed arc connecting such nodes indicates that one of the corresponding markings may be transformed into another one by firing of a transition. In this way each arc in the reachability graph corresponds to a transition. The reachability graph of an unbounded net is infinite. A net is bounded if there exists an upper bound of the token number for all places in all states of the net. If a net is bounded in every initial marking it is called *structurally bounded*.

A transition is called *dead* in a state if no marking is reachable anymore to enable this transition to fire. A transition is *live* in a given marking if it is not dead in any reachable marking. A net is *live* if all transitions in the initial marking are live. A state of the net is *dead* if no transition can fire anymore. Based on the reachability graph some dynamic net properties like liveness and reversibility can be decided. A net is *reversible*, i.e. resettable, if the initial marking can be reached again from any reachable marking of the net.

The net's incidence matrix  $C$  is an  $(m \times n)$ -matrix, where each entry  $c_{ij}$  states the token change on the place  $p_i$  by firing of the transition  $t_j$ , i.e.  $c_{ij} = O(t_j, p_i) - I(p_i, t_j)$ , see the input and output functions above. Using this matrix, a *p-invariant* is defined by a vector  $y \in \mathbb{N}^m$  satisfying the equation

$$y \cdot C = 0. \quad (1)$$

The invariant entries which are unequal to zero define the support of the invariant, denoted for invariant  $y$  as  $\text{supp}(y)$ . For a *p-invariant* it indicates which places are contained in this invariant.

A *t-invariant* is defined by a vector  $x \in \mathbb{N}^n$  satisfying the equation

$$C \cdot x = 0. \quad (2)$$

An invariant is called *minimal* if it does not contain any other invariant by its support and if the greatest common divisor of all its support entries is one. A net is *covered by t-invariants* (*p-invariants*) if each transition (place) is contained in an invariant.

A *trap* is a set of places, whose all output transitions are also input transitions of that set. A trap is maximal if it is not a proper subnet of any other trap. A *deadlock* is a non-empty set of places, whose all input transitions are also output transitions of that set. A deadlock is minimal if it does not properly contain any other deadlock.

In graphical representations the construct of *logical nodes* avoids an immoderate arc crossing. If a node is defined as being a logical one, it is identified with every other logical node with the same name and hence these nodes have the same ID. A logical node may occur in different copies in the model being logically identical.

### 3.2. Time dependent models

In order to model some time dependencies of the body iron homeostasis process the Petri nets have been extended by adding a time interval to each place (cf. [28]). Such a net will be called *deterministic interval timed places Petri net* (DITPPN).

In our model a time interval  $[\tau_i, \tau'_i]$  is associated with each place  $p_i$ . It means a token has to stay at place  $p_i$  not less than  $\tau_i$  and not more than  $\tau'_i$  units of time before it can be removed from that place. Only after that time the token is available. In other words, the token has to stay at place  $p_i$  for some time before it will be able to flow to its post-transition. This time is not given as a single value. Instead, an interval containing the actual value of this time (which is not a priori known) is given. It should be emphasized that after time  $\tau'_i$  (which is measured relative to the time when the token arrived at place  $p_i$ ) the token may, but not has to flow to the post-transition. The token will flow when the tokens from other pre-places of the transition will be also available.

In the concept of classical time Petri nets a time interval  $[\tau_i, \tau'_i]$  is associated with each place  $p_i$ . Let us consider a token which is put on place  $p_i$  at time  $t$ . As in our concept the token is not available before  $t + \tau_i$ . But in a time Petri net the token has to be removed before  $t + \tau'_i$  otherwise it will be a wasted object and called a dead token which cannot be used anymore. So, the sojourn in some state of a time Petri net must have a value between the minimal and the maximal value.

In the concept of timed Petri nets to each place  $p_i$  a duration  $d_i$  is assigned. Each token has to remain at least  $d_i$  time units at place  $p_i$  before it is available. Obviously, a timed Petri net with given durations  $d_i$  can be transformed into a time Petri net by associating the interval  $[d_i, \infty]$  to each place. For further information about the concepts of time and timed Petri nets see [29].

Each place in a DITPPN models a certain possible action or process, for instance a data processing or a message transmission. It can be considered as a condition which must be fulfilled in order to start some biochemical reaction. The duration of that processing or transmission is described by the interval  $[\tau, \tau']$ . The interval bounds are non-negative real numbers.

The meaning of the time intervals is as follows. After the start of a processing or a transmission (or some biochemical process) which is modeled by the arrival of a token to the place, the end of the processing or the transmission occurs not earlier than at time  $\tau$  and not later than at time  $\tau'$ .

The token may be removed from a place by the firing of its post-transition only. It means that when the transition does not fire the token stays in its pre-place waiting for conditions allowing its 'consumption', i.e. firing the transition. From this follows that the token can stay in the place after time  $\tau'$  (i.e. the right bound of the interval) waiting for firing its post-transition.

When two places  $p_1$  and  $p_2$  with the associated intervals  $[\tau_1, \tau'_1]$  and  $[\tau_2, \tau'_2]$ , respectively, support the firing of a transition, then the firing time of this transition falls into the interval  $[\max\{\tau_1, \tau_2\}, \max\{\tau'_1, \tau'_2\}]$  (if we assume that the tokens arrived to these places at time  $t = 0$ ). When one of the processes supporting an event ends earlier, the outcome (result) of this process waits for the outcome of the second process, and when the second process ends its execution, then the event immediately occurs (in the model it is expressed by the firing of a transition). If both processes end their execution at the same time then the transition is fired immediately.

When the transition fires in a given time interval (depending on the time intervals of its pre-places) then the remaining firing times of other transitions in the net should be recalculated, taking into account the actual firing time of the transition which has just fired.

The deterministic interval timed places Petri net (DITPPN) can be formally defined as a 6-tuple  $(P, T, I, O, M_0, F_\tau)$ , where

- $(P, T, I, O, M_0)$  is a Petri net, and
- $F_\tau : P \rightarrow [\mathbb{R}^+ \cup \{0\}, \mathbb{R}^+ \cup \{0\}]$  is a function which associates places with deterministic time intervals.

The rules of DITPPN need a bit more explanations. It should be noticed that the firing of a transition is an atomic action. After the firing the tokens are removed from its pre-places and put at its post-places. The firing only may occur if the transition is enabled. The transition is enabled, if all its pre-places possess the required number of tokens and all times associated with tokens have been expired (which means that in the case of each pre-place the token is present in it for at least  $\tau$  time units, where  $\tau$  is the left bound of the time interval associated with the place).

In general, time intervals are associated with places, however it means further, that time intervals may be associated with tokens. Let us consider for example a channel in which we have two instances of the same message, e.g. an acknowledgment. Both of them may have initially the same interval associated. However, after some steps of a Petri net execution, both intervals may differ, because the first token participates in the Petri net execution, but the second one does not yet.

Let us assume that there is a transition  $t_1$  with two pre-places  $p_1$  and  $p_2$  and one post-place  $p_3$ . The time interval associated with  $p_1$  is  $[\tau_1, \tau'_1]$  and the interval associated with  $p_2$  is  $[\tau_2, \tau'_2]$ . It means that transition  $t_1$  will fire in the relative time interval  $[\max\{\tau_1, \tau_2\}, \max\{\tau'_1, \tau'_2\}]$ . So, in this interval a token flows into the post-place  $p_3$ .

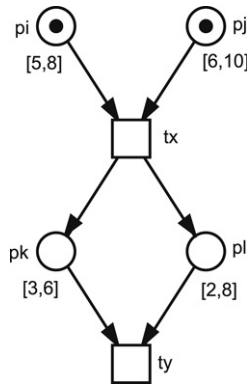


Fig. 1. An example of a simple DITPPN.

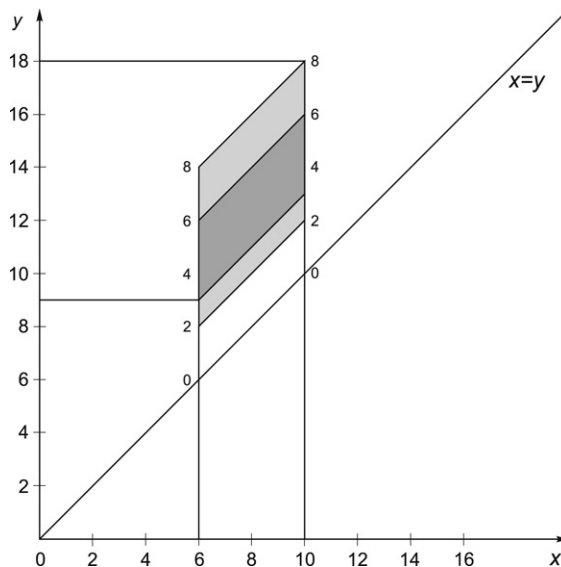


Fig. 2. The polygons corresponding to the time interval of firing the transition  $t_y$  from Fig. 1. The light-grey polygon corresponds to the place  $pl$ , and the dark-grey one corresponds to the  $pk$  (note that the dark one is “included” in the light one). Since the transition  $t_x$  fires in the time interval  $[6, 10]$  (denoted in the  $x$ -axis) the places  $pk$  and  $pl$  receive tokens in this interval. Place  $pk$  has to keep a token between 3 and 6 time units. Similarly, place  $pl$  releases its token in time interval  $[2, 8]$  relative to the time of receiving it. Hence, transition  $t_y$  fires in the time interval  $[9, 18]$ .

The time of the firing of transition  $t_1$  is selected from the interval  $[\max\{\tau_1, \tau_2\}, \max\{\tau'_1, \tau'_2\}]$ . These times are not specified by a probability distribution. The only values which are specified are lower and upper bounds of the interval.

Let us note that during the evolution of the system both the entry time to a state and the exit time from the state are in the form of intervals. It means that if the state of a system is described using a Cartesian coordinate system in which the abscissa denotes the entry time to a state and the ordinate denotes the exit time from the state, then the time of the occurrence of an event is of the form of a polygon [28,30]. This observation is a basis of an analysis method which can be applied to the DITPPNs. The main idea of the method is illustrated in Figs. 1 and 2. In the first of them a simple net is shown. In this net the transition  $t_x$  fires in time interval  $[\max\{5, 6\}, \max\{8, 10\}] = [6, 10]$  (here it is assumed that the entry times of the tokens to the pre-places of transition  $t_x$  are equal to the time when the analysis of the system starts, but in general each time is relative). Hence, the places  $pk$  and  $pl$  receives their tokens in the same interval (it should be emphasized that the exact times of the token receiving by these places is impossible to determine in advance, hence these times have to be described by the intervals). Then the transition  $t_y$  fires in the time interval  $[\max\{2, 3\}, \max\{6, 8\}] = [3, 8]$ , but this is an interval of relative time. In order to obtain an absolute time interval its bounds should be increased by adding the bounds of the time interval which describes the time, when the transition  $t_x$  fires, i.e.  $[6, 10]$ . As a result an interval  $[3 + 6, 8 + 10] = [9, 18]$  is obtained (see Fig. 2).

4. Results and discussion

In the following, the time dependent Petri net model of the human body iron homeostasis is introduced. Afterwards, some analysis results are presented which verify the net’s structure.

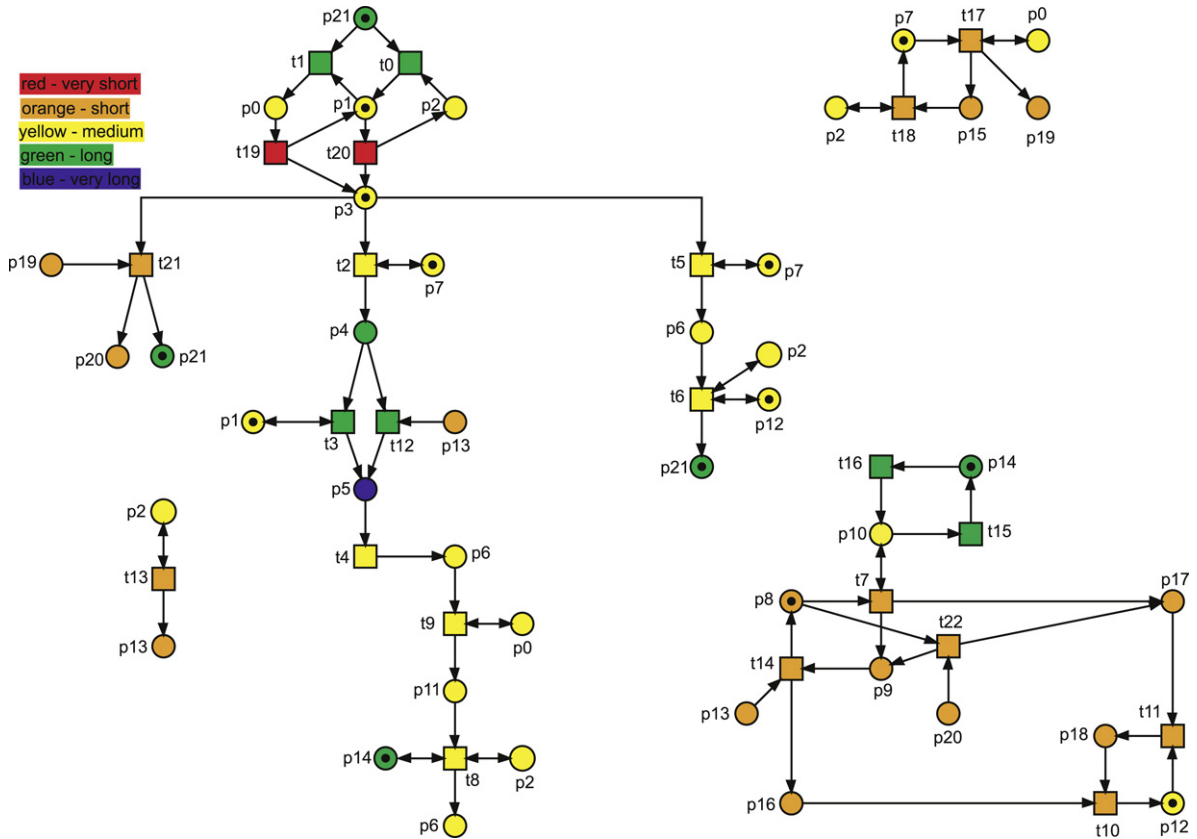


**Fig. 3.** The Petri net modeling the processes of human body iron homeostasis. Time labeling of the nodes is encoded in different colors. The durations of the different time intervals is given in Table 2.

4.1. The time dependent model of the human body iron homeostasis

The model of the body iron homeostasis process presented in this paper is an extension of the core of the model introduced and analyzed in [2–4]. In the model each biochemical reaction is described by a transition and conditions necessary to start such a reaction correspond to some places of the Petri net. However, in that model any information of time dependencies between its components is not included. In the extension presented here this information is modeled by time intervals associated with places. They should be interpreted as periods of time during which a particular biochemical condition associated with a given place has to be fulfilled in order to enable some reaction modeled by its post-transition. More precisely, the left bound of such an interval corresponds to the minimal time during which some biochemical condition has to be fulfilled, while the right bound corresponds to the maximal required time of the fulfillment. After that time the token is available for the post-transitions firing but it may also stay there longer.

The above explained approach of analyzing the DITPPN with a time polygon based method requires the examination of the systems states. Therefore, it makes sense to restrict the state space of the model. The former model, discussed in [2–4], is an unbounded one, i.e. its state space is infinite. According to that, one main goal of the model refinement is to restrict the systems state space to arrive at a finite one without splitting too much of the former model that means to keep as much of its verified biological features as possible. The structural and dynamic properties of the new Petri net model as well as its time extensions are presented in the next section. The new model is graphically presented in Fig. 3. Its transitions and places are listed in Tables 1 and 3, respectively. Since the exact time dependencies between the components of the homeostasis process are not known, in the model five different time intervals approximating the actual values have been used. They are listed in Table 2.

The place *p5*, erythrocyte, is assigned with the interval *very long* since it is known that the erythrocytes are endocytosed in the one-nuclear cells after 100–120 days. Since it is biologically more intuitive to assign time intervals to the reactions, i.e. transitions, we first assign time intervals to these and based on that, the places' time intervals are derived depending on the duration of their adjacent transitions (compare Tables 1 and 3, respectively).

4.2. Analysis of the model without time

To verify the structure of the model as well as its qualitative behavior independent of time, the Petri net firstly is analyzed without the extension of the time intervals. This analysis is performed according to the approach applied in [3]. There, the

**Table 1**

The 23 transitions of the model are listed with their IDs and their names. The right column contains the assigned time interval of the transitions. A specification of the intervals is given in Table 2.

ID	Name	Time interval
0	Increasing low Fe level	Long
1	Increasing medium Fe level	Long
2	Endocytosis in preerythrocyte(RME)(TfR1)	Medium
3	Erythrocyte synthesis	Long
4	Phagocytosis in one-nuclear cell	Medium
5	Endocytosis in one-nuclear cell (RME)(TfR1)	Medium
6	Transport out of one-nuclear cell	Medium
7	Hepcidin increase(expressed in liver)	Short
8	(Fe2+) release	Medium
9	Store(Apoferritin)(IRP)	Medium
10	Fpn increase	Short
11	Fpn decrease/inhibition	Short
12	Erythrocyte synthesis	Long
13	Signal EPO synth in kidney	Short
14	Hepcidin inhibition	Short
15	Regeneration	Long
16	Inflammation process	Long
17	TfR1 inhibition(RNAdegradation via IRP)	Short
18	TfR1 synthesis(RNAstabilisation via IRP)	Short
19	Binding Tf	Very short
20	Binding Tf	Very short
21	Tf(Fe3+)+TfR2	Short
22	Hepcidin increase(expressed in liver)	Short

**Table 2**

The specification of the time intervals assigned to the nodes of the model.

Abbr.	Interval	Time duration
vs	Very short	[0 s; 30 s]
s	Short	[1 min; 5 min]
m	Medium	[2 h; 5 h]
l	Long	[2 days; 5 days]
vl	Very long	[100 days; 120 days]

**Table 3**

The 22 places of the model are listed with their IDs and their names. The middle columns name their pre- and post-transitions whose assigned intervals are given as abbreviations in brackets. The right column contains the assigned time interval (cf. Table 2) of the places; if they are not unambiguous given by the intervals of their adjacent transitions they are written in quotation marks. For each logical place the superscript number <sup>n</sup> names the number of copies of this places in Fig. 3. The subscript numbers <sub>n</sub> indicate how many tokens a place carries in the initial marking.

ID	Name	Adjacent transitions		Time interval
		Pre-transitions	Post-transitions	
0	Fe serum high <sup>3</sup>	1 (l), 9 (m), 17 (s)	9 (m), 17 (s), 19 (vs)	"Medium"
1	Fe serum medium <sub>1</sub> <sup>2</sup>	0 (l), 3 (l), 19 (vs)	1 (l), 3 (l), 20 (vs)	"Medium"
2	Fe serum low <sup>5</sup>	6 (m), 8 (m), 13 (s), 18 (s), 20 (vs)	0 (l), 6 (m), 8 (m), 13 (s), 18 (s)	"Medium"
3	Tf(Fe3+) <sub>1</sub>	19 (vs), 20 (vs)	2 (m), 5 (m), 21 (s)	"Medium"
4	Hem(Fe2+)	2 (m)	3 (l), 12 (l)	"Long"
5	Erythrocyte	3 (l), 12 (l)	4 (m)	Very long
6	LIP <sup>3</sup>	4 (m), 5 (m), 8 (m)	6 (m), 9 (m)	Medium
7	TfR1 <sup>3</sup>	2 (m), 5(m), 18(s)	2 (m), 5 (m), 17 (s)	"Medium"
8	Less hepcidin <sub>1</sub>	14 (s)	7 (s), 22 (s)	Short
9	Much hepcidin	7 (s), 22 (s)	14 (s)	Short
10	Inflammation	7 (s), 16 (l)	7 (s), 15 (l)	"Medium"
11	(Fe3+) Ferritin	9 (m)	8 (m)	Medium
12	Much Fpn <sub>1</sub> <sup>2</sup>	6 (m), 10 (s)	6 (m), 11 (s)	"Medium"
13	Much EPO <sup>3</sup>	13 (s)	12 (l), 14 (s)	"Short"
14	No inflammation <sub>1</sub> <sup>2</sup>	8 (m), 15 (l)	8 (m), 16 (l)	"Long"
15	Less TfR1	17 (s)	18 (s)	Short
16	Positive Fpn Signal	14 (s)	10 (s)	Short
17	Negative Fpn Signal	7 (s), 22 (s)	11 (s)	Short
18	Less Fpn	11 (s)	10 (s)	Short
19	TfR2 <sup>2</sup>	17 (s)	21 (s)	Short
20	Free HFE <sup>2</sup>	21 (s)	22 (s)	Short
21	Fe3+ in serum <sub>1</sub> <sup>3</sup>	6 (m), 21 (s)	0 (l), 1 (l)	"Long"

**Table 4**

The minimal  $p$ -invariants of the model. Place  $p_0$  in the third invariant is marked with a superscript <sup>2</sup>. This is the only entry of the minimal  $p$ -invariants which is unequal to one, i.e. here it is two.

$p$ -invariant	Places	Biological meaning
1	0, 1, 2	Iron level in serum
2	8, 9	Hepcidin level
3	$0^2$ , 1, 3, 4, 5, 6, 11, 21	Iron pathway through erythrocyte and one-nuclear cell
4	12, 18	Fpn level
5	10, 14	State of inflammation
6	7, 15	TFR1 level

**Table 5**

In the model used read arcs cause the processing of the  $t$ -invariants. These ones containing transitions of the right column (these are connected with empty places via read arcs in the net) without containing the transitions on the left-hand side have to be merged to  $t$ -invariants containing the transitions of the left column.

Transitions providing tokens	Transitions requiring tokens
1	9, 17
16	7
20	6, 8, 13, 18

model is presented and analyzed which serves as a basis of the model presented here. During the development of this current model all structural properties are kept. That means the Petri net is ordinary and also homogeneous, it is not pure, not conservative and not statically conflict-free. It is neither bounded nor structurally bounded. As discussed below in detail, the model is covered with  $t$ -invariants but not with  $p$ -invariants. It has six minimal  $p$ -invariants which are exactly the six minimal deadlocks of the net. The net holds the deadlock-trap-property. This means the maximal trap in each minimal deadlock is sufficiently marked, i.e. it contains a place which carries sufficiently many tokens, so that all its post-transitions may fire. Therefore, the net has no dead reachable states [31]. To the contrary to the former model, the new one is not only connected but also strongly connected since the ways of iron uptake are not taken into account anymore.

#### 4.2.1. Invariant analysis

Over the places of a  $p$ -invariant the weighted sum of tokens is constant independently of any transitions firing, see Eq. (1). Therefore, the minimal  $p$ -invariants are applied in metabolic networks as substrate conservations [32]. In the model presented in this paper the minimal  $p$ -invariants are used as a kind of switcher indicating e.g. different concentration levels of the represented species.

The net contains six minimal  $p$ -invariants listed in Table 4, where the right column contains their biochemical meaning. To ensure that the  $p$ -invariants contribute to the net behavior, each of them carries a token in the initial marking, see the subscript numbers in Table 3. Apart from the third listed one, all minimal  $p$ -invariants contain exactly one token and explicitly represent a kind of switcher embedded as a subnet in the model. The third minimal  $p$ -invariant contains more than one token. Over its places there circulates the weighted sum of three tokens. As marked in Table 4, a token at place  $p_0$  is weighted by the factor 2. Considering Fig. 3 this is comprehensible. Thus, the places of that invariant carry three tokens already in the initial marking. All the tokens in the initial marking are put into the net in the way that the corresponding marked places represent an inactive state, respectively the initial marking represents the system state being assumed to be the physiologically normal one.

Each minimal  $t$ -invariant, see Eq. (2), gives a multiset of transitions whose common firing reproduces a marking. Considering the initial marking, they provide flows through the net leading again to this marking. Thus, the  $t$ -invariants stand for crucial sub-processes in the homeostasis process modeled by the net. In [33] the minimal  $t$ -invariants are named to represent the basic behavior of the system.

The model is covered by its eleven minimal  $t$ -invariants. Some read arcs are used in the model and cannot be realized in the incidence matrix as node connections. Therefore, they are not taken into account in the incidence matrix based calculation of the  $t$ -invariants. Generally, there are approaches dealing with non-pure nets, e.g. [34] proposes a net transformation of non-pure nets into pure ones. This transformation refers to subnets in which a transition is connected to a pre-place which is also a post-place but the arcs of these connections are differently weighted. In contrary to that, our model is ordinary, i.e. also the arcs of the loops are equally weighted with 1.

Thus, we process the minimal  $t$ -invariants to get some feasible ones. The feasibility of the  $t$ -invariants is a necessary criterion for their realizability in the initial marking. According to [35] the procedure is as follows. During the processing those  $t$ -invariants are searched which contain transitions connected with an empty place via a read arc without containing transitions which provide tokens on that place. These found  $t$ -invariants are merged with such ones providing the mentioned tokens. Table 5 names the corresponding transitions. The processing provides 22 feasible  $t$ -invariants presented in Table 6. Transitions which occur only in the same feasible  $t$ -invariants build a so-called maximal common transition set, i.e. MCT-set [35], see Table 7, with its own biological meaning. To improve the overview over the feasible  $t$ -invariants in order to check their biological meaning, the feasible  $t$ -invariants are clustered according to their contained transitions [36]. Firstly,

**Table 6**

The 22 feasible  $t$ -invariants transitions of the model. Table 7 lists which transitions are contained in the MCT-sets.

No.	Involved transitions		No.	Involved transitions	
	Single transitions	MCT-sets		Single transitions	MCT-sets
1	–	6	12	12, 13	1, 2, 3, 4, 5, 7
2	12, 13,	1, 3	13	3, 12, 13	1, 2, 3, 4
3	3	1, 3	14	5, 12, 13	1, 2, 3, 4
4	5	1	15	3, 12, 13	1, 2, 3, 4, 5, 7
5	12, 13	1, 2, 3, 5, 7	16	5, 12, 13	1, 2, 3, 4, 5, 7
6	3, 12, 13	1, 2, 3	17	3, 5, 12, 13	1, 2, 3, 4
7	5, 12, 13	1, 2, 3	18	3, 13	1, 2, 3, 4, 5, 7
8	3, 13	1, 2, 3, 5, 7	19	3, 5, 13	1, 2, 3, 4, 5, 7
9	5, 13	1, 2, 5, 7	20	5, 13	1, 2, 4, 5, 7
10	3, 12, 13	1, 2, 3, 5, 7	21	3, 7, 13	1, 3, 5, 6
11	5, 12, 13	1, 2, 3, 5, 7	22	5, 7, 13	1, 5, 6

**Table 7**

The MCT-sets of the model. The transitions building one of these sets occur only in form of that set in the feasible  $t$ -invariants. Therefore, the MCT-sets represent some biologically meaningful functional units, see the right column.

MCT-sets	Contained transitions	Biological meaning
1	0, 6, 20	Low iron level caused iron release from LIP
2	1, 19	High iron level
3	2, 4	Iron pathway through erythrocyte
4	8, 9	Iron store
5	10, 11, 14	Fpn regulation, hepcidin increase caused by EPO
6	15, 16	Inflammatory and regeneration process
7	17, 18, 21, 22	TfR1 and TfR2 regulation with increasing of free HFE

**Table 8**

The 22 feasible  $t$ -invariants of the model clustered by UPGMA (70%). The two columns on the right-hand list the processes contained in the clusters, split into occurring MCT-sets and single transitions. The integers in brackets indicate with which percentage this process is contained in the cluster's invariants. No specification means 100% occurrence of the corresponding transition(-s) in the cluster. The column to the left of this gives the total number of invariants in the cluster.

Cluster no.	No. of invariants	Contained processes	
		MCT-sets	Single transitions
1	2	1, 3(50), 5, 6	3(50), 5(50), 7, 13
2	11	1, 2, 3(82), 4(55), 5, 7	3(45), 5(45), 12(55), 13
3	1	1	5
4	1	1, 3	3
5	5	1, 2, 3, 4(60)	3(60), 5(60), 12, 13
6	1	1, 3	12, 13
7	1	6	–

the distance matrix  $D$  for the  $t$ -invariants is calculated. In our approach we consider the distance matrix based on the feasible  $t$ -invariants. According to [37] the distance measure  $d_{ij}$  for two feasible  $t$ -invariants  $x_i$  and  $x_j$  is defined as  $d_{ij} = 1 - s(x_i, x_j)$  where the similarity measure  $s(x_i, x_j)$  is the Tanimoto coefficient, i.e. for two  $t$ -invariants  $x_i, x_j$  it satisfies the equation [38]:

$$s(x_i, x_j) = \frac{|supp(x_i) \cap supp(x_j)|}{|supp(x_i) \cup supp(x_j)|}. \tag{3}$$

Using the distance matrix, the feasible  $t$ -invariants are clustered. For that purpose the UPGMA approach is a proper agglomerative hierarchical clustering algorithm: in each iteration the two most similar clusters are merged. Here, the distance  $\Delta_{kl}$  between two clusters  $C_k$  and  $C_l$  is given by the average distance of all possible pairs of their invariants, i.e. the distance is given by the equation

$$\Delta_{kl} = \frac{1}{|C_k| \cdot |C_l|} \cdot \sum_{x_i \in C_k, x_j \in C_l} d_{ij}. \tag{4}$$

Generally, the algorithm terminates when all clusters are joined in one cluster.

In the following the clusters for the model are presented with an accordance of 70% within a cluster. This provides seven clusters, listed in Table 8 and shown in Fig. 4 (produced by means of [1]).

The clusters 1 to 7 all contain MCT-set 1 representing an iron release from the LIP. The first two clusters contain an Fpn regulation (MCT-set 5) and an EPO increase (transition  $t$ 13). The last-mentioned process is additionally contained in the clusters 5 and 6, in which the increased EPO level supports the erythrocyte synthesis (transition  $t$ 12). The TfR is regulated

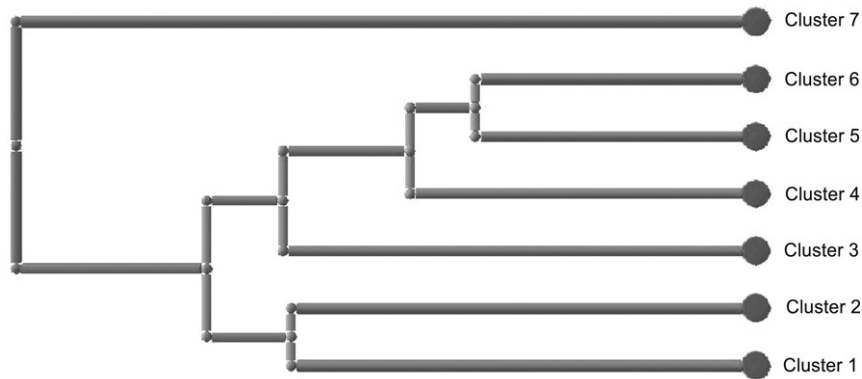


**Fig. 4.** The 22 feasible  $t$ -invariants built seven UPGMA based clusters with an accordance of 70% within each cluster. For more information see Table 8. This figure was produced using [1].

**Table 9**

The places of the model with their assigned capacities.

Place ID	Capacity	Place ID	Capacity
0	1	11	3
1	1	12	1
2	1	13	2
3	3	14	1
4	3	15	1
5	3	16	2
6	3	17	2
7	1	18	1
8	1	19	2
9	1	20	2
10	1	21	3

(MCT-set 7) only in cluster 2. The clusters 2 and 5 are the only ones including a high iron level in serum (MCT-set 2) and in some of their  $t$ -invariants a storage of iron by means of Ferritin (MCT-set 4).

All clusters 4 to 6 and several  $t$ -invariants of the clusters 1 and 2 contain the iron pathway through an erythrocyte (MCT-set 3). Accordingly, some of them contain an EPO independent erythrocyte synthesis (transition  $t_3$ ), especially those of them which do not include an EPO supported synthesis (see above). All  $t$ -invariants of cluster 3 and some of the clusters 1, 2 and 5 comprise an iron transport directly in the one-nuclear cell (transition  $t_5$ ).

Cluster 7 consists only of the inflammatory and the regeneration process (MCT-set 6). Apart from this cluster, these processes are also contained in cluster 1 which thus is the only one containing an inflammation caused hepcidin regulation (transition  $t_7$ ).

All these clusters are biologically meaningful. It should be also noticed that the applied reduction method based on MCT-sets and clustering is a general approach and can be applied also for much larger nets, where the reduction should be more significant (cf. [3]).

#### 4.2.2. Bounded model

As mentioned above the time polygon analysis approach is based on the system states. Therefore, it makes sense to restrict the state space. But as above mentioned the model in the former form is unbounded. To restrict the number of reachable states a special capacity is assigned to each place, i.e. the place cannot carry more than an assigned integer number of tokens. Table 9 contains the places and their capacities. All places contained in minimal  $p$ -invariants which use as a kind of switcher only one token circulating between the places of the invariant get a capacity of one. The remaining places of the minimal  $p$ -invariant 3 of Table 4 each gets a capacity of three since three tokens are circulating in that  $p$ -invariant. For convenience a capacity of two is assigned to all remaining places. That should be large enough not to restrict the net dynamics but small enough not to produce too many states, i.e. nodes in the reachability graph.

After introducing these capacities the Petri net is bounded. Thus, it is possible to calculate the reachability graph and based on this decide some dynamic properties of the net including these capacities.

The net is not covered by  $p$ -invariants and hence it is not structurally bounded. The model has no dead transitions in the initial marking and no dead reachable states. The net is live. Its reachability graph is strongly connected and thus the net is reversible. Summarizing those dynamic net properties, the system is able to return from every reachable marking to the initial one, that means that the physiologically normal system state can be recreated, the goal of the iron homeostasis process. There is no modeling error which could cause an unintended interruption of the processes since the net is live.

## 5. Conclusions

In the paper a time dependent Petri net based model of the human body iron homeostasis process has been presented. It is an extension of the recently proposed model of that important biochemical process. The extension includes time features of the iron homeostasis. This is an important addition since some of the time dependencies existing within the process (i.e. between some components of it) may be crucial for understanding this phenomenon. We have included time intervals to places since the exact durations which are needed in real life to enable a reaction to take place are not known. For that purpose we have introduced a new variant of time depending Petri nets, the DITPPN. An analysis of a DITPPN including the time information is very complex. Thus, we present a time independent analysis which verifies the structural net properties as well as the net behavior without taking into account the time. Furthermore, we present a possible way of analyzing the time properties with the polygon based method. Until now, a complete analysis based on this approach is still inefficient. But an improvement of this approach is a subject of our future research.

## References

- [1] WiDa - Wilmascope for Distance Analysis, <http://nwg.bic-gh.de/wida>.
- [2] D. Formanowicz, A. Sackmann, P. Formanowicz, J. Blazewicz, Petri net based model of the body iron homeostasis, *J. Biomed. Inform.* 40 (2007) 476–485.
- [3] A. Sackmann, D. Formanowicz, P. Formanowicz, I. Koch, J. Blazewicz, An analysis of the Petri net based model of the human body iron homeostasis process, *Comput. Biol. Chem.* 31 (2007) 1–10.
- [4] D. Formanowicz, A. Sackmann, P. Formanowicz, J. Blazewicz, Some aspects of the anemia of chronic disease modeled and verified by Petri net based approach (submitted for publication).
- [5] C.A. Petri, Communication with automata, in: *Schriften des IIM Nr. 3, Institut für Instrumentelle Mathematik* (1962) Bonn, pp. 16–27 (in German).
- [6] R. Hofestädt, A petri net application of metabolic processes, *J. Syst. Anal. Modell. Simul.* 16 (1994) 113–122.
- [7] V.N. Reddy, M.L. Mavrovouniotis, M.N. Liebman, Petri net representation in metabolic pathways, in: *Proc. Int. Conf. Intell. Syst. Mol. Biol.* 1993, pp. 328–336.
- [8] K. Voss, M. Heiner, I. Koch, Steady state analysis of metabolic pathways using Petri nets, *Silico Biol.* 3 (2003) 367–387.
- [9] A. Doi, S. Fujita, H. Matsuno, M. Nagasaki, S. Miyano, Constructing biological pathway models with hybrid functional Petri nets, *Silico Biol.* 4 (2004) 271–291.
- [10] H. Matsuno, Y. Tanaka, H. Aoshima, A. Doi, M. Matsui, S. Miyano, Biopathways representation and simulation on hybrid functional petri net, *Silico Biol.* 3 (2003) 389–404.
- [11] S. Hardy, P.N. Robillard, Modelling and simulation of molecular biology systems using Petri nets: Modelling goals of various approaches, *J. Bioinform. Comput. Biol.* 2 (2004) 595–613.
- [12] J.W. Pinney, D.R. Westhead, G.A. McConkey, Petri net representations in systems biology, *Biochem Soc Trans* 31 (2003) 1513–1515.
- [13] K. Lautenbach, Exact liveness conditions of a petri net class, *GMD Report 82*, Bonn, 1973 (in German).
- [14] S. Schuster, C. Hilgetag, R. Schuster, Determining elementary modes of functioning in biochemical reaction networks at steady state, in: *Proc. Second Gauss Symposium* 1993, 1996, pp. 101–114.
- [15] M. Heiner, I. Koch, Petri net based system validation in systems biology, in: *Proc. ICATPN 2004*, in: *LNCS*, vol. 3099, Bologna, 2004, pp. 216–237.
- [16] R.R. Crichton, *Inorganic Biochemistry of Iron Metabolism*, Ellis Horwood Ltd, West Sussex, 1991.
- [17] Y. Beguin, Soluble transferrin receptor for the evaluation of erythropoiesis and iron status, *Clin. Chim. Acta* 329 (2003) 9–22.
- [18] C. Enns, A. Sussman, Physical characterization of the transferrin receptor in human placenta, *J. Biol. Chem.* 256 (1981) 9820–9823.
- [19] A. Jacobs, Low molecular weight intracellular iron transport compounds, *Blood* 50 (1977) 433–439.
- [20] R. Oria, X. Alvarez-Hernández, J. Licéaga, J.H. Brock, Uptake and handling of iron from transferrin, lactoferrin and immune complexes by a macrophage cell line, *Biochem. J.* 9 (1998) 221–225.
- [21] P. Aisen, C.A. Enns, M. Wessling-Resnick, Chemistry and biology of eucariotic iron metabolism, *Int. J. Biochem. Cell. B.* 33 (2001) 940–995.
- [22] T. Ganz, Hepcidin, a key regulator of iron metabolism and mediator of anemia and inflammation, *Blood* 102 (2003) 783–788.
- [23] G.J. Anderson, D.M. Frazer, Hepatic iron metabolism, *Semin. Liver. Dis.* 25 (2005) 420–432.
- [24] D.M. Frazer, G.J. Anderson, The orchestration of body iron intake: How and where do enterocytes receive their cues, *Blood Cells Mol. Dis.* 30 (2003) 288–297.
- [25] T. Murata, Petri nets: Properties, analysis and applications, *Proc. of the IEEE* 77 (1989) 541–580.
- [26] W. Reisig, *Petri Nets: An Introduction*, Springer Verlag, Heidelberg, 1985.
- [27] J. Wang, *Timed Petri Nets. Theory and Applications*, Kluwer Academic Publishers, Boston, 1998.
- [28] J. Brzeziński, M. Sajkowski, A polygon time structure for protocol verification, in: *Proc. Parallel Processing and Applied Mathematics Conference*, Kazimierz Dolny, Poland, September 14–17, 1999, pp. 177–194.
- [29] R. David, H. Alla, *Discrete, Continuous, and Hybrid Petri Nets*, Springer Verlag, Heidelberg, 2005.
- [30] J. Brzeziński, M. Sajkowski, Detection of livelocks in communication protocols by means of a polygon time structure, in: *Proc. 19th Symp. on Reliable Distributed Systems*, 2000, pp. 84–93.
- [31] P.H. Starke, *Analysis of Petri Net Models*, Teubner Verlag, Stuttgart, 1990 (in German).
- [32] I. Zevedei-Oancea, S. Schuster, Topological analysis of metabolic networks based on Petri net theory, *Silico Biol.* 3 (2003) 323–345.
- [33] M. Heiner, I. Koch, J. Will, Model validation of biological pathways using Petri nets - demonstrated for apoptosis, *Biosystems* 75 (2004) 15–28.
- [34] K. Lautenbach, Linear algebraic techniques for place/transition nets, advances in petri nets petri nets (1986), pp. 142–167.
- [35] A. Sackmann, M. Heiner, I. Koch, Application of Petri net based analysis techniques to signal transduction pathways, *BMC Bioinform.* 7 (2006) 482.
- [36] PInA - Petri net Invariant Analyser, <http://www-dssz.informatik.tu-cottbus.de/>.
- [37] E. Grafahrend-Belau, F. Schreiber, M. Heiner, A. Sackmann, B.H. Junker, S. Grunwald, A. Speer, K. Winder, I. Koch, Modularization of biochemical networks based on classification of Petri net  $t$ -invariants, *BMC Bioinform.* 9 (2008) 90.
- [38] K. Backhaus, B. Erichson, W. Plinke, R. Weiber, *Multivariate Analysis Methods. An Application-Oriented Introduction*, 10th ed., Springer, Berlin, 2000 (in German).